Signal Processing 137 (2017) 149–159

Contents lists available at ScienceDirect

Signal Processing

journal homepage: www.elsevier.com/locate/sigpro

# Maneuvering target imaging and scaling by using sparse inverse synthetic aperture

Gang Xu[a,b], Lei Yang[a,c], Guoan Bi[a,*], Mengdao Xing[d]

[a] School of Electrical and Electronic Engineering, Nanyang Technological University, 50 Nanyang Avenue, 639798, Singapore
[b] State Key Laboratory of Millimeter Waves, Southeast University, Nanjing, 210096, China
[c] Tianjin Key Laboratory for Advanced Signal Processing, Civil Aviation University of China, Tianjin, 300300, China
[d] National Laboratory of Radar Signal Processing, Xidian University, Xi'an, 710071, China

ARTICLE INFO

*Article history:*
Received 20 October 2016
Revised 7 January 2017
Accepted 17 January 2017
Available online 9 February 2017

*Keywords:*
Inverse synthetic aperture radar (ISAR)
Sparse aperture (SA)
Maneuvering targets
Motion estimation

ABSTRACT

In recent years, there have been increasing interests in addressing the issue of high-resolution inverse synthetic aperture radar (ISAR) imaging from sparse aperture (SA) data. The non-uniform rotation property of maneuvering target introduces non-stationary echo modulation to exhibit two-dimensional (2-D) migration through resolution cells (MTRC), which increases the difficulty of SA-ISAR imaging. In this paper, we focus on ISAR imaging and scaling of maneuvering target for effective MTRC correction and SA synthesis. Under a scaled non-uniform Fourier dictionary to include MTRC, SA maneuvering target imaging is formatted as sparse representation with maximum a posterior (MAP) estimation. Then, sparse ISAR imaging joint with parameter estimation is solved by using a two-step procedure. The estimated rational parameters are used to rescale the reconstructed ISAR image to extract the 2-D target geometry. Finally, the experiments based on simulated and measured data are performed to confirm the effectiveness of the proposed algorithm.



## 1. Introduction

Inverse synthetic aperture radar (ISAR) has the capability of providing two-dimensional (2-D) high-resolution images of non-corporative moving targets, which has become an important tool in remote sensing [1–6]. To achieve high-resolution imaging in the cross-range dimension, ISAR needs to acquire continuous sampling with a large aspect angle variation between radar and the targets, which, however, may hardly be satisfied in some practical applications [7–9]. Generally, a multi-functional radar system has to provide the capabilities of searching, detecting, tracking and imaging multiple targets. The system resources need to be optimally allocated for different tasks using a time-sharing mechanism. In this case, transmitting and collecting the wide-band signal pulses in a continuous long-time duration may be infeasible for ISAR imaging due to the constraints from multi-task operations. For example, the radar beam needs to scan at a slow speed to track the observed target by transmitting narrow-band signal pulses. As a result, the wide-band measurements are discontinuously forming sparse aperture (SA). The multi-source interferences also tend to introduce corruptions in the echo data [8]. Furthermore, the measurements collected from multiple sensors of diverse angle distribution tend to be discontinuous in a network radar system [9]. Therefore, the task of SA data synthesis or spectrum estimation for high-resolution ISAR imaging is essential to promote the development of modern radar system.

To effectively suppress the artifacts due to data incompletion, many different techniques of SA data spectrum estimation have been proposed over the last few decades. In general, the existing methods can be categorized into the following three groups.

- Modern spectrum estimation: The missing data are interpolated and extrapolated based on the parametric [10,11] or non-parametric [12,13] spectrum estimation. Because it is assumed that the measurement geometry is known or deterministic, the methods in this group are more or less sensitive to model errors.
- CLEAN methods: The image formation is treated as a deconvolution processing to iteratively decompose the SA data by extracting the main-lobes of major Doppler responses as scattering centers [14,15]. These methods are usually efficient but sensitive to noise.
- Sparse signal recovery: Sparse representation of ISAR image with an over-complete dictionary is utilized for full-aperture (FA) imaging [16–28]. Such a sparse method is more tolerant to

* Corresponding author.
*E-mail addresses:* gangxu@seu.edu.cn (G. Xu), l_yang@cauc.edu.cn (L. Yang), egbi@ntu.edu.sg (G. Bi), xmd@xidian.edu.cn (M. Xing).

http://dx.doi.org/10.1016/j.sigpro.2017.01.016
0165-1684/

model errors and is robust to effectively suppress the noise corruption for desirable performance improvement over the methods in the previous two groups.

For maneuvering target, its rotational velocity is usually time variant during a long coherent processing interval (CPI) and tends to induce 2-D migration through resolution cells (MTRC) in ISAR image [29–33]. The range MTRC behaves as non-uniform range shifts while the cross-range MTRC exhibits spatial-variant Doppler modulation in the phase history domain. Because MTRC increases with the increment of 2-D resolution, its correction is necessary for high-resolution imaging. In FA case, some effective methods [28–32] have been proposed to deal with MTRC. Unfortunately, most of the existing methods are invalid in SA case. During recent years, some works have been reported to resolve the 2-D MTRC correction in sparse ISAR imaging [22,25,33]. Our previous work in [33] has designed a 2-D MTRC-included dictionary based on the assumption that the rotational parameters are known and can be estimated before SA-ISAR imaging. In fact, it is still a challenge to accurately estimate the rotational parameters from the SA data. In [22], a parametric sparse representation approach is presented by repeating ISAR image reconstruction on different sets of rotational parameters, which requires a high computational load. In fact, the computational efficiency of sparse ISAR imaging can be improved if we can provide reliable initial value of rotational parameters. It is worth mentioning that our previous work in [25] presents an efficient sparse ISAR imaging algorithm by two-step procedure. In [25], coarse rotational parameter estimation is firstly realized by using an entropy minimization method, and then sparse ISAR imaging joint with more accurate parameter estimation is achieved by solving a parametric sparse representation problem. When coarse rotational parameter estimation is available, the algorithm proposed in [25] can effectively promote computational efficiency. Taking into account that our previous work in [25] is only applicable for non-maneuvering targets of uniform rotation, we extend it to the case of maneuvering target in this paper. The main contributions of our work in this paper are listed as follows:

- The SA signal model of maneuvering target is investigated and a scaled non-uniform Fourier dictionary is constructed to represent the 2-D MTRC.
- The two-step procedure in [25] is modified to be suitable for SA-imaging and rotational parameter estimation of maneuvering targets.
- Experimental analysis based on simulated and measured data is performed to show the effectiveness of the proposed algorithm in dealing with the target maneuverability in SA-ISAR imaging.

The rest of the paper is organized as follows. In Section 2, the SA image formation of maneuvering target is introduced from a statistically sparse perspective. The two steps of the proposed SA-ISAR imaging method are presented in Section 3.1 and 3.2, respectively. In Section 4, experiments using the simulated and measured data are performed to validate the effectiveness of the proposed algorithm in achieving the ISAR image of maneuvering target.

## 2. ISAR image formation of maneuvering target

The ISAR imaging geometry is shown in Fig. 1 that the rotational motion of the target forms the sampling patterns of inverse synthetic array. As shown in Fig. 1, the target rotation is decomposed into two orthogonal components. One is around $Y$ axis, i.e., the direction of line of sight (LOS) from radar to the mass center $O$ of the target. For a target of 2-D rotation, the other component is constant around $Z$ axis during the CPI. Then, the imaging plane is determined as the $X$-$O$-$Y$ plane. It is assumed that the translational motion of the target has already been successfully compensated [17,18,26,34,35]. Then, the instantaneous range from scatterer

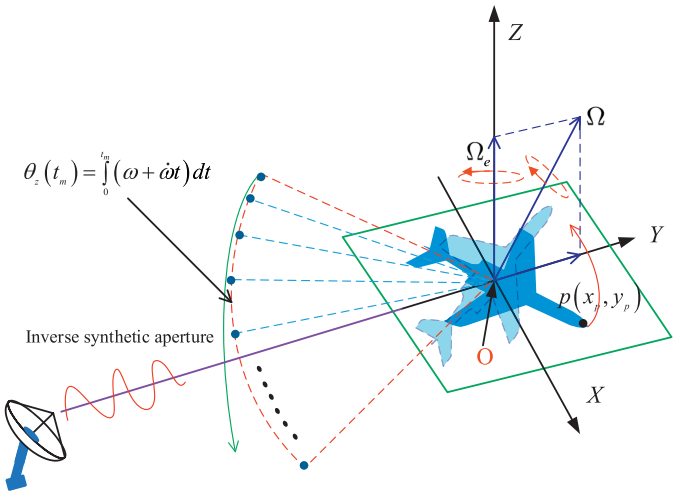


**Fig. 1.** ISAR imaging geometry.

$p$ at the position of $(x_p, y_p)$ to radar is expressed as [28]

$$R_p(t_m) = R_0 + \cos\theta_z(t_m)\cdot y_p + \sin\theta_z(t_m)\cdot x_p \tag{1}$$

where $t_m \in [-M/2+1 : M/2]/PRF$ is the dwell time, $PRF$ is the pulse repetition frequency (PRF), $M$ is the number of pulses for FA, and $\theta_z(t_m)$ is the rotational angle around $Z$ axis. Different from our previous work in [25], we consider a maneuvering target with non-uniform rotation. In such a case, the rotational angle becomes $\theta_z(t_m) = \omega t_m + \dot{\omega}t_m^2/2 + O(t_m^2)$, where $\omega$ and $\dot{\omega}$ are the angular speed and acceleration, respectively. Then, (1) is approximated by using Taylor series expansion [29] as

$$R_p(t_m) \approx R_p - y_p\cdot\omega^2 {t_m}^2/2 + x_p\cdot\left(\omega t_m + \dot{\omega}t_m^2/2 + O\left(t_m^2\right)\right) \tag{2}$$

where $R_p = R_0 + y_p$. For simplicity, only the angular acceleration is considered here by neglecting the higher order terms. Even though, the proposed algorithm is still suitable for a target with higher order maneuverability and the deduction is straightforward.

Assuming that the radar system transmits pulses of linear frequency modulation (LFM) signal, the range compression/imaging is applied using the matched filter technique [24]. From (2), the range compressed data are expressed as

$$S(\hat{t};t_m) \approx \iint_{(x_p,y_p)\in object} \sigma_p\cdot\mathrm{sinc}\left(B\left(\hat{t}-2\frac{R_p+x_p\omega t_m}{c}\right)\right) \cdot\exp\left[-j4\pi f_c\frac{R_p+x_p\omega t_m+\kappa_p {t_m}^2/2}{c}\right]dx_p dy_p \tag{3}$$

where $\kappa_p = x_p\dot{\omega} - y_p\omega^2$, $\sigma_p$ is the scattering coefficient of scatterer $p$, $\mathrm{sinc}(\hat{t}) = \sin(\pi\hat{t})/\hat{t}$, $\hat{t}$ denotes the fast time in the slant-range dimension, $B$ and $f_c$ are the bandwidth and carrier frequency of the transmitted signal, respectively, and $c$ represents the transmitting speed of the electromagnetic wave. In (3), only the linear range shift in the envelope is reserved for the range-MTRC because the quadratic term is too small to induce the range-MTRC [28]. The chirp/quadratic phase in (3) corresponds to the cross-range-MTRC, which can be decomposed into the range-dependent and cross-range-dependent components [29]. Then, (3) is transformed into range frequency domain as

$$S(f_r,t_m) \approx \iint_{(x_p,y_p)\in object} \tilde{S}_p(f_r,t_m)\cdot\exp\left[j2\pi f_c\frac{y_p\omega^2 {t_m}^2}{c}\right]dx_p dy_p$$
$$\tilde{S}_p(f_r,t_m) = \sigma_p\cdot\exp\left[-j2\pi\frac{f_c+f_r}{c}(2R_p+(2\omega+\dot{\omega}t_m)\cdot x_p t_m)\right]. \tag{4}$$